

Chaotic and turbulent temperature fluctuations in atmospheric free convection

A. Bershadskii
ICAR, P.O. Box 31155, Jerusalem 91000, Israel

It is shown, using results of direct numerical simulations, laboratory experiments, measurements in the atmospheric boundary layer and satellite infrared radiances data, that the temperature fluctuations in atmospheric free convection can be well described by the distributed chaos approach based on the Bolgiano-Obukhov phenomenology.

I. INTRODUCTION

At free convection the fluid or gas are driven by the density fluctuations produced by temperature (humidity) differences (see, for instance, Ref. [1]). The mean flows in forced convection can drastically change the fluid dynamics and result in non-universality of the observed spectra of the atmospheric temperature fluctuations. The pure free convection conditions are rarely observed in atmosphere. On the other hand, one can expect that the free convection can be characterized by universal types of the spectra. Therefore, the atmospheric free convection (in the atmospheric boundary layer, for instance, see Refs. [2],[3] and references therein) can be used for the fundamental studies of the buoyancy driven turbulence, providing a firm basis for understanding of the more frequently observed forced convection. Moreover, the near free convection can play a significant role in the large-scale atmospheric motions where the winds can be considered as a natural part of the buoyancy driven atmospheric convection itself.

The deterministic chaos in the atmospheric motions was also discovered on a simple model of free convection [4] (see for a recent review Ref. [5]). In present paper the deterministic chaos approach has been generalized on the case with randomly fluctuating parameters and takes the form of distributed chaos, that allows consideration of thermal convection with large Rayleigh (Reynolds) numbers typical for atmosphere. This consideration is based on the Bolgiano-Obukhov phenomenology [6]-[9] and supported by comparison with direct numerical simulations, laboratory experiments and atmospheric measurements.

In Section II the free convection in the Boussinesq approximation and the Kolmogorov-Bolgiano-Obukhov approach for the inertial-buoyancy range have been considered both for unstable and stable stratification. In Section III the Bolgiano-Obukhov distributed chaos has been introduced. In Section IV results of laboratory experiments for large Rayleigh numbers have been discussed and compared with the predictions made for the Bolgiano-Obukhov distributed chaos. In Section V these predictions have been compared with results of measurements made in the atmospheric boundary layer (over sea and land) and with results of satellite infrared radiances measurements over a planetary-scale tropic area.

II. FREE CONVECTION

The buoyancy driven convection in the Boussinesq approximation is described by equations [10]

$$\frac{\partial \mathbf{u}}{\partial t} + (\mathbf{u} \cdot \nabla) \mathbf{u} = -\frac{\nabla p}{\rho_0} + \sigma g \theta \mathbf{e}_z + \nu \nabla^2 \mathbf{u} \quad (1)$$

$$\frac{\partial \theta}{\partial t} + (\mathbf{u} \cdot \nabla) \theta = S \frac{\Delta}{H} e_z u_z + \kappa \nabla^2 \theta, \quad (2)$$

$$\nabla \cdot \mathbf{u} = 0 \quad (3)$$

where θ is the temperature fluctuations over a temperature profile $T_0(z)$, p is the pressure, \mathbf{u} is the velocity, \mathbf{e}_z is a unit vector along the gravity direction, g is the gravity acceleration, H is the distance between the layers and Δ is the temperature difference between the layers, ρ_0 is the mean density, ν is the viscosity and κ is the thermal diffusivity, σ is the thermal expansion coefficient. For the unstable stratification $S = +1$ and for the stable stratification $S = -1$.

These equations at $\nu = \kappa = 0$ have an invariant

$$\mathcal{E} = \int_V (\mathbf{u}^2 - S \sigma g \frac{H}{\Delta} \theta^2) d\mathbf{r} \quad (4)$$

where V is the spatial volume (see, for instance, Ref. [10]).

Then, corresponding generalization of the Kolmogorov-Bolgiano-Obukhov approach for the inertial-buoyancy range of the spatial scales [8] provides a relationship between characteristic temperature fluctuations θ_c and the characteristic wavenumber scale k_c

$$\theta_c \propto (\sigma g)^{-1} \varepsilon^{2/3} k_c^{1/3} \quad (5)$$

where the generalized dissipation rate

$$\varepsilon = \left| \frac{d \langle \mathbf{u}^2 - S \sigma g \frac{d}{\Delta} \theta^2 \rangle}{dt} \right| \quad (6)$$

$\langle \dots \rangle$ denotes spatial averaging.

When the buoyancy forces dominate over the inertial forces (see for the stable stratification Ref. [8] and for the unstable one Refs. [11]-[13]) one can use

$$\varepsilon_b = \left| \frac{d\langle \theta^2 \rangle}{dt} \right| \quad (7)$$

instead of the ε and then one obtains

$$\theta_c \propto (\sigma g)^{-1/5} \varepsilon_b^{2/5} k_c^{1/5} \quad (8)$$

instead of the relationship Eq. (5).

III. DISTRIBUTED CHAOS

For the bounded and smooth dynamical systems the exponential frequency spectrum

$$E(f) \propto \exp(-f/f_c) \quad (9)$$

is usually associated with deterministic chaos (see, for instance, Refs. [14]-[18]).

For the spatial (wavenumber) domain this spectrum is replaced by the spectrum

$$E(k) \propto \exp(-k/k_c) \quad (10)$$

(see, for instance, Ref. [14] and references therein).

In the buoyancy driven unstably stratified thermal convection at the Prandtl number $Pr = \nu/\kappa \sim 1$ transition to turbulence occurs at the Rayleigh number $Ra \sim 10^6$ [19]. Figure 1 shows (in the log-log scales) power spectrum of temperature fluctuations at $Pr = 1$ and $Ra = 6.6 \times 10^6$ obtained in a direct numerical simulation reported in Ref. [20] (the spectral data were taken from the Fig. 11 of the Ref. [20]). Two branches of this spectrum correspond to different number of the Fourier modes: the upper branch to a small number whereas the lower branch corresponds to the most of the modes. Therefore, the only lower one has a physical significance. The dashed curve in the Fig. 1 indicates the exponential spectrum Eq. (10). The dotted arrow indicates position of the k_c .

Transition to turbulence usually results in fluctuations of the parameter k_c . These fluctuations can be taken into account by an ensemble averaging

$$E(k) \propto \int_0^\infty P(k_c) \exp(-(k/k_c)) dk_c \propto \exp(-(k/k_\beta)^\beta) \quad (11)$$

The stretched exponential in the right-hand side of the Eq. (11) is generalization of the exponential spectrum Eq. (10). An estimation of the asymptotic (at large k_c) behaviour of the probability distribution $P(k_c)$

$$P(k_c) \propto k_c^{-1+\beta/[2(1-\beta)]} \exp(-\gamma k_c^{\beta/(1-\beta)}) \quad (12)$$

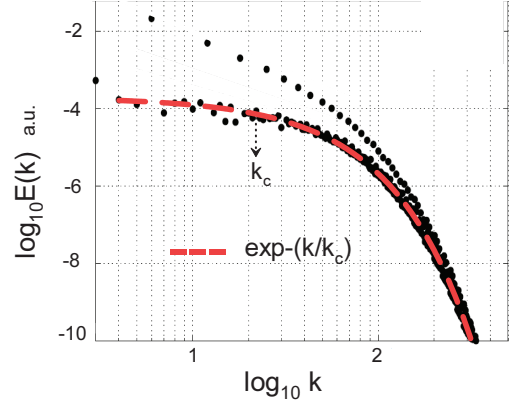


FIG. 1: Power spectrum of the temperature fluctuations at $Pr = 1$ and $Ra = 6.6 \times 10^6$ (onset of the convective turbulence).

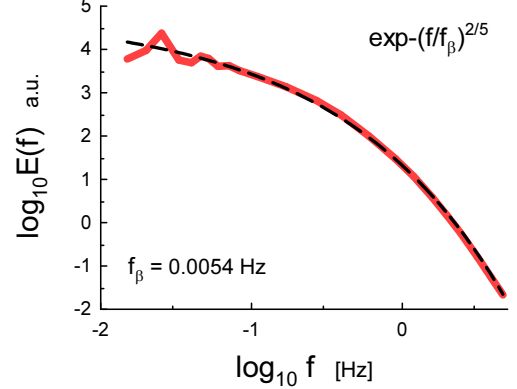


FIG. 2: Power spectrum of the experimentally observed temperature fluctuations at $Pr = 0.8$ and $Ra = 1.35 \times 10^{14}$.

(where γ is a constant) can be made from the Eq. (11) [21].

The Eqs. (5) and (8) can be considered in a general form

$$\theta_c \propto k_c^\alpha \quad (13)$$

When θ_c has a Gaussian distribution [8] relationship between parameters α and β

$$\beta = \frac{2\alpha}{1+2\alpha} \quad (14)$$

follows immediately from the Eqs. (12-13).

For the Eq. (5) $\alpha = 1/3$, hence $\beta = 2/5$ and

$$E(k) \propto \exp(-(k/k_\beta)^{2/5}). \quad (15)$$

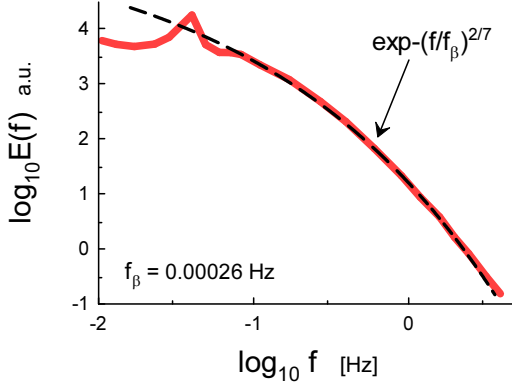


FIG. 3: The same as in Fig. 2 but for $Ra = 2.05 \times 10^{11}$.

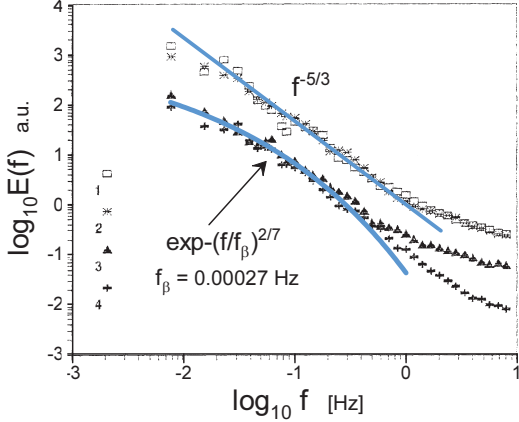


FIG. 4: Four power spectra of the temperature fluctuations in the atmospheric surface layer over sea at near free convection conditions.

For the Eq. (8) $\alpha = 1/5$, hence $\beta = 2/7$ and

$$E(k) \propto \exp - (k/k_\beta)^{2/7}, \quad (16)$$

IV. LABORATORY EXPERIMENTS

In the laboratory experiments the frequency spectra are usually obtained instead of the wavenumber ones. Figure 2, for instance, shows power spectrum of the experimentally observed temperature fluctuations for the Rayleigh-Bénard convection (unstable stratification) in a cylindrical cell with $Pr = 0.8$ and at very high Rayleigh number $Ra = 1.35 \times 10^{14}$ (the spectral data were taken from Fig. 2 of the Ref. [22]).

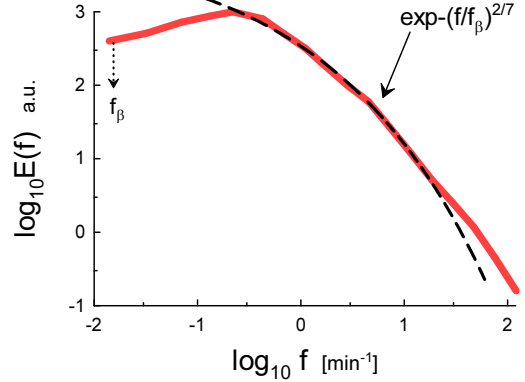


FIG. 5: Power spectra of the temperature fluctuations in the atmospheric surface layer over land at near free convection conditions.

This is a frequency spectrum. However, in the case of free convection the mean flow velocity U_0 , usually used for the Taylor hypothesis [8],[14] relating f and k : $f = U_0 k/2\pi$, can be replaced by a characteristic velocity of advection by the energy-containing eddies past the probe [23],[24] (see also Ref. [25] and references therein) and we should compare this spectrum with the Eq. (15). The dashed curve in the Fig. 2 indicates correspondence to the stretched exponential Eq. (15).

Figure 3 shows power spectrum of the temperature fluctuations observed in analogous experiment but for considerably smaller Rayleigh number $Ra = 2.05 \times 10^{11}$. The dashed curve in the Fig. 3 indicates correspondence to the stretched exponential Eq. (16).

V. ATMOSPHERIC THERMAL CONVECTION

The Ref. [2] reports results of measurements of the temperature fluctuations in the near free convection (at unstable stratification) by a fixed probe over sea surface (the height of the tower was ~ 12 m above the sea surface). The weather was calm and the sea surface was aerodynamically smooth. In the air the r.m.s. horizontal velocity fluctuations were comparable to the wind gusts. Results for four data sets obtained during a day were reported: two with comparatively high temperature fluctuations and two with low ones. Figure 4 shows the four power spectra of the temperature fluctuations corresponding to the four data sets (the spectral data were taken from Fig. 1c of the Ref. [2]). The solid straight line is drawn to indicate the $^{-5/3}$ power law for the strong fluctuations case [8], whereas the curved solid line is drawn to indicate the stretched exponential

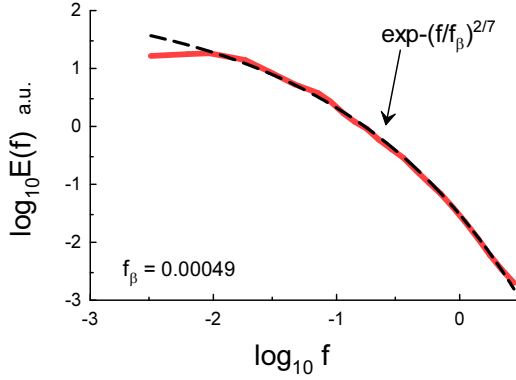


FIG. 6: Power spectra of the alongwind-sampled temperature fluctuations in the unstable atmospheric surface layer over ocean.

Eq. (16) for the weak fluctuations case (see previous Section about applicability of the Taylor hypothesis for the free convection).

The Ref. [3] reports results of measurements of the temperature fluctuations in the near free convection over land. The measurements were produced by 'Eddy-covariance' tower (at 2.29m height) and Sodar/RASS system in the morning hours (from 07:35 to 08:40 UTC) over a corn field. Moderate to high buoyancy fluxes and a drop of the wind speed result in domination of buoyancy over shear. The occurrence of large-scale turbulence structures (plumes) were registered. The free convection conditions occur at about 50 percent of the 92 days of the measurement period. Figure 5 shows power spectrum of the temperature fluctuations (the sonic spectral data were taken from Fig. 6h of the Ref. [3]). The dashed line is drawn to indicate the stretched exponential Eq. (16) and the dotted arrow indicates position of f_β .

It is well known (although not well understood) that the free-like convection behaviour can be often observed under conditions which seems to be rather different from the free ones. Figure 6, for instance, shows power spectrum of the temperature fluctuations airborne measured in the Weastern Atlantic ocean at 50m level above the water surface during cold air outbreaks [26]. The measurements were made in near-shore areas of roll vortices and cloud streets under considerable mean wind shear. The alongwind-sampled spectral data were taken from Fig. 4 of the Ref. [26] (f is the frequency normalized by Z/V_a , where Z is the height and V_a is the relative velocity between the aircraft and air). The dashed line is drawn to indicate the stretched exponential Eq. (16).

The geostationary satellite infrared radiances data for spatial range of scales from 100km up to 5000km can

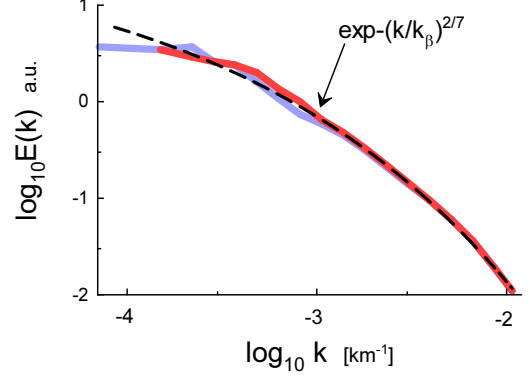


FIG. 7: Power spectra of the MTSAT satellite thermal infrared radiances (the two different colors correspond to zonal and meridional spectra).

also be viewed as a result of a nearly free convection. At this case the winds can be approximately considered as an internal part of the large-scale thermal convection, especially for geographical scenes located not too far from the equator where the Coriolis forces can be neglected as well.

Figure 7 shows wavenumber power spectrum corresponding to these conditions (the spectral data were taken from Fig. 2 of Ref. [27]). The spectra were computed using 1386 images from the infrared channel sensitive to temperature at the top of clouds over area with longitudes 80°E-200°E and latitudes 40°S-30°N and with resolution 30 km. The data were obtained by the geostationary MTSAT satellite (see Ref. [28] and references therein). The dashed line in the Fig. 7 is drawn to indicate the stretched exponential Eq. (16).

VI. CONCLUSIONS

The Bolgiano-Obukhov phenomenology appears to be adequate for the atmospheric free convection in the atmospheric boundary layer (both over land and sea) when it is considered in the frames of the distributed chaos approach. Moreover, it can be also applied to the atmospheric data for the temperature fluctuations even in some cases when the free convection conditions are not satisfied and over the large-scale tropic areas when the winds can be considered as a part of the planetary-scale convection (though the radiative processes should be also taken into account in this case).

[1] T. Foken, *Micrometeorology* (Springer, Berlin-Heidelberg, 2008)

[2] A.A. Grachev, *Boundary-Layer Meteorology*, **69**, 27 (1994)

[3] R. Eigenmann, S. Metzger, and T. Foken, *Atmos. Chem. Phys.*, **9**, 8587 (2009)

[4] E.N. Lorenz, *J. Atmos. Sci.*, **20**, 130 (1963)

[5] S. Vannitsem, *Chaos*, **27**, 032101 (2017)

[6] R. Bolgiano, *J. Geophys. Res.*, **64**, 2226 (1959)

[7] A.M. Obukhov, *Dokl. Akad. Nauk SSSR*, **125**, 1246 (1959)

[8] A. S. Monin, A. M. Yaglom, *Statistical Fluid Mechanics*, Vol. II: *Mechanics of Turbulence* (Dover Pub. NY, 2007)

[9] E.S.C. Ching, *Statistics and Scaling in Turbulent Rayleigh-Bénard Convection* (Singapore: Springer, 2014)

[10] A. Kumar, A.G. Chatterjee and M.K. Verma, *Phys. Rev. E*, **90**, 023016 (2014)

[11] I. Procaccia and R. Zeitak, *Phys. Rev. Lett.*, **62**, 2128 (1989)

[12] V.S. L'vov, *Phys. Rev. Lett.*, **67**, 687 (1991)

[13] G. Falkovich and V.S. L'vov, *Physica D*, **57**, 85 (1992)

[14] J. E. Maggs and G. J. Morales, *Phys. Rev. Lett.*, **107**, 185003 (2011); *Phys. Rev. E* **86**, 015401(R) (2012); *Plasma Phys. Control. Fusion*, **54**, 124041 (2012)

[15] N. Ohtomo, K. Tokiwano, Y. Tanaka et. al., *J. Phys. Soc. Jpn.*, **64**, 1104 (1995)

[16] D.E. Sigeti, *Phys. Rev. E*, **52**, 2443 (1995)

[17] J. D. Farmer, *Physica D*, **4**, 366 (1982).

[18] U. Frisch and R. Morf, *Phys. Rev.*, **23**, 2673 (1981)

[19] M.K. Verma, *Scholarpedia*, **14**, 53051 (2019)

[20] P.K. Mishra and M.K. Verma, *Phys. Rev. E*, **81**, 056316 (2010)

[21] D.C. Johnston, *Phys. Rev. B*, **74**, 184430 (2006)

[22] X. He, D. van Gils, E. Bodenschatz, and G. Ahlers, *Proc. 15th European Turbulence Conference* (2015), <http://etc15.fyper.com/proceedings/proceedings/documents/189.pdf>

[23] H. Tennekes, *J. Fluid Mech.*, **67**, 561 (1975)

[24] A. Kumar and M.K. Verma, *R. Soc. open sci.*, **5**, 172152 (2018)

[25] A. Bershadskii, *Chaos* **20**, 043124 (2010)

[26] S.H. Chou and E.N. Yen, *J. Atmos. Sci.*, **44**, 3721 (1987)

[27] J. Pinel, S. Lovejoy, D. Schertzer, *Atmos. Res.*, **140-141**, 95 (2014)

[28] W. Takeuchi, T. Nemoto, T. Kaneko, Y. Yasuoka, *Asian J. Geoinf.*, **10**, 29 (2010)